

# A COMPONENT MODE SYNTHESIS APPROACH FOR DYNAMIC ANALYSIS OF ELASTOMER DAMPING DEVICES

J.-F. Deü<sup>1</sup>, B. Morin<sup>1</sup>, A. Legay<sup>1</sup>

<sup>1</sup> LMSSC, Conservatoire National des Arts et Métiers, 2 rue Conté, 75003 Paris, France, jean-francois.deu@cnam.fr

*Abstract: In the context of passive damping, various mechanical systems from aerospace or automotive industries use elastomer components (shock absorbers, silent blocks, flexible joints, etc.). The frequency and temperature dependence of the constitutive behavior of these devices, as well as their complex geometries, lead to costly numerical models. The aim of this work is to propose reduced order models of elastomer damping devices taking into account their complex geometries and their dissipative material behavior. A finite element model of 3D rubber dampers is firstly developed using a fractional derivative viscoelastic constitutive model identified from Dynamic Mechanical Analysis (DMA). An efficient reduced model is then derived from this FE model by using an original extension of the sub-structuring Craig-Bampton method in the case of viscoelastic damping. This approach consists in choosing a combination of static and dynamic modes, the latter being obtained from real eigenvalue problems adapted for highly damped structures. Moreover, the super-element is defined by considering that the device's interfaces are much more rigid than the rubber core. Consequently, a kinematical constraint is employed to enforce rigid body motion of the sub-structure interfaces. The combination of these techniques leads to a twelve degrees-of-freedom super-element replacing the initial full model. As an application, the dynamic response of a structure supported by four hourglass shaped rubber devices under harmonic loads is analyzed to show the efficiency of the proposed approach.*

**Keywords:** *damping joints, viscoelasticity, substructuring approach, reduced order model*

## INTRODUCTION

Due to their capacities to dissipate energy, elastomers are highly used in damping devices like silent blocs or joints. A typical example of this use is found in the spatial industry: during takeoff and flight, launchers are subject to a significant amount of vibrations from either the propulsion engine or the acoustical environment. Shocks may also occur during the pyrotechnic separation of the different floors of the launcher. All these vibration sources may damage the satellite or any other sensitive equipment onboard, and a common solution is to use viscoelastic damping devices to dissipate a part of the mechanical energy.

The design of these damping devices is usually done by using the finite element method. The computational cost of the associated models may become prohibitive for example during an optimization process. Many solutions already exist to reduce the numerical model of linear undamped structures, but only a few give access to reduced order models with damping behavior, especially when it comes from viscoelasticity which may be seen as a strong form of damping. Two types of solutions for the reduction of viscoelastic models can be found in the literature. The first one consists in the replacement of the damping device model by an equivalent rheological model which can be identified through a series of experimental measurements on the damper. The main problem with this approach is that the behavior of the rheological model may not fit the real behavior of the damper in all directions, and more importantly necessitate experimental identification for each new device and consequently can't be used for optimization purpose. The second one, which is chosen in this work, is to use a finite element model of the damper and to achieve the reduction using a substructuring based for example of the Craig-Bampton method.

The original Craig-Bampton method (Craig and Bampton, 1968) uses a combination of static and dynamic modes to reduce the finite element model of a sub-structure to a smaller finite element model called super-element. Here we propose a modified Craig-Bampton method taking into account the frequency dependence of the mechanical properties. This approach, based upon the work of Rouleau, Deü and Legay (2014), consists in choosing a modal projection basis well adapted to highly damped structures. Moreover, the super-element is obtained by considering that the device's interfaces are much more rigid than the rubber core. To make use of this difference, a kinematical constraint is employed to enforce rigid body motion of the sub-structure interfaces (Morin, Legay and Deü, 2016). The combination of all these techniques leads to a twelve dofs super element (three rotations and three translations per face) replacing the initial full model. As an application, the dynamic response of a structure supported by four hourglass shaped rubber devices under harmonic loads is analyzed to show the efficiency of the proposed approach.

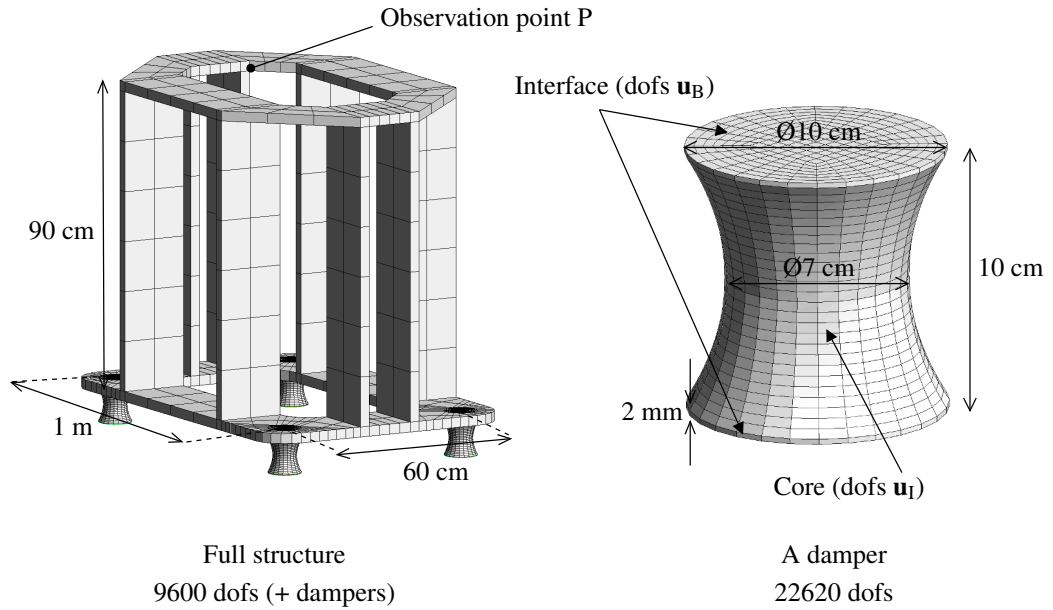


Figure 1 – Full structure mounted on four dampers, and details of a damper

## PROBLEM UNDER STUDY AND VISCOELASTIC MODEL

The complete model is composed of a support structure mounted on four hourglass shaped dampers, as seen on Fig. 1. The support structure is made of aluminum and the dampers are made of two aluminum thin interface plates and an elastomer core. Two different material models are used in this work: a linear elastic Hooke's model is chosen for the aluminum, and a viscoelastic fractional derivative model, initially proposed by Bagley and Torvik (1983), is chosen for the elastomer. In this paper, the four-parameter fractional Zener model is considered to define the complex frequency dependent shear modulus  $G^*(\omega)$ :

$$G^*(\omega) = \frac{G_0 + G_\infty(i\omega\tau)^\alpha}{1 + (i\omega\tau)^\alpha} \quad (1)$$

where  $G_0$  and  $G_\infty$  are respectively the static modulus  $G_0 = G^*(\omega \rightarrow 0)$  and the high frequency limit of the dynamic modulus  $G_\infty = G^*(\omega \rightarrow \infty)$ ,  $\tau$  is the relaxation time and  $\alpha$  is the order of the fractional derivative. More information about this model, its identification and its finite element implementation in time domain can be found in (Galucie, Deü, Ohayon, 2004).

In the frequency domain, the finite element model can be written in the following form:

$$\left( \mathbf{K}^e + \mathbf{K}_{\text{sph}}^v + \frac{G^*(\omega)}{G_0} \mathbf{K}_{\text{dev}}^v - \omega^2 \mathbf{M} \right) \mathbf{u} = \mathbf{f} \quad (2)$$

where  $\mathbf{M}$  is the mass matrix,  $\mathbf{K}^e$  is the purely elastic part of the stiffness matrix which is assembled on the aluminum interfaces dofs and  $\mathbf{K}^v$  is the viscoelastic part of the stiffness matrix which is assembled on the elastomer core dofs.

In the previous equation, the viscoelastic stiffness matrix is separated into a spheric part  $\mathbf{K}_{\text{sph}}^v$  and a deviatoric part  $\mathbf{K}_{\text{dev}}^v$ . This separation is used due to the fact that the viscoelastic behavior of elastomer is mainly caused by distortional strain (not by volume change). The adimensional viscoelastic modulus  $G^*(\omega)/G_0$  is also used in the dynamic equation to clearly show that the frequency dependence appears only in a scalar function, all the matrices being real and frequency-independent. Since the deviatoric stiffness matrix is the only matrix subjected to the complex modulus  $G^*(\omega)$ , the dynamic equation can also be expressed in terms of a static stiffness matrix  $\mathbf{K}^0$  and a frequency dependent stiffness matrix  $\mathbf{K}^\infty$ :

$$\left( \mathbf{K}^0 + i\omega h^*(\omega) \mathbf{K}^\infty - \omega^2 \mathbf{M} \right) \mathbf{u} = \mathbf{f} \quad (3)$$

where  $\mathbf{K}^0 = \mathbf{K}^e + \mathbf{K}_{\text{sph}}^v + \mathbf{K}_{\text{dev}}^v$  and  $\mathbf{K}^\infty = (G_\infty/G_0 - 1) \mathbf{K}_{\text{dev}}^v$  and where  $h^*(\omega)$  is a dimensionless frequency dependent modulus:

$$h^*(\omega) = \frac{\tau^\alpha (i\omega)^\alpha}{1 + (i\omega\tau)^\alpha} \quad (4)$$

The material parameters used to build the mass and stiffness matrices are given in Tab. 1 for the aluminum and Tab. 2 for the elastomer. The structure is composed of 7540 nodes for each rubber damper, which is enough to get converged results in the frequency range of interest, and 3200 nodes for the upper aluminum structure. Only the computational cost of the dampers model is studied and reduced here, so the mesh of the upper structure is kept small for convenient computation

time. Each damper represents 22620 dofs. The total number of dofs in the complete structure is about  $10^5$ , including more than 90% for the dampers only, thus underlining the need for an efficient reduction method. The finite element code for this study is an in house program developed in both Python and Fortran. The finite elements are 8 nodes hexahedra anywhere in the structure. Rubber dampers are connected to the aluminum structure through their upper interface.

**Table 1 – Material parameters of the aluminum.**

Parameters	Values
E	70 GPa
$\nu$	0.3
$\rho$	2700 kg·m <sup>-3</sup>

**Table 2 – Material parameters of the elastomer.**

Parameters	Values
E	0.947 MPa
$\nu$	0.45
$\rho$	1000 kg·m <sup>-3</sup>
$G_0$	0.327 MPa
$G_\infty$	0.126 GPa
$\alpha$	0.3
$\tau$	0.52 $\mu$ s

## MODEL ORDER REDUCTION

Two reduction steps are used in this study. The first one is a kinematical constraint that makes use of the difference of stiffness between the rubber core and the aluminium interface of the dampers. This constraint is used to reduce the interface dofs. The second step consists in the reduction and the condensation of the internal dofs of the elastomer core to their previously reduced interface dofs.

### Rigid interfaces assumption

Due to the difference between the aluminum and the elastomer stiffness, the aluminum interfaces may be considered to be rigid compared to the rubber core. A kinematic constraint is used to enforce the rigid body motion of the interfaces. The velocity of any point A of an interface can be written in terms of the velocity of the center C of the same interface and the cross-product of the distance between point A and point C and the rotation  $\Omega$  of the interface. This relationship can be extended to the displacement within the context of small displacement, namely:

$$\vec{u}_A = \vec{u}_C + \vec{AC} \times \vec{\Omega} \quad (5)$$

In matrix form, the same constraint is written by:

$$\begin{bmatrix} u_A \\ v_A \\ w_A \end{bmatrix} = \begin{bmatrix} 1 & 0 & 0 & 0 & (z_A - z_C) & (y_C - y_A) \\ 0 & 1 & 0 & (z_C - z_A) & 0 & (x_A - x_C) \\ 0 & 0 & 1 & (y_A - y_C) & (x_C - x_A) & 0 \end{bmatrix} \begin{bmatrix} u_C \\ v_C \\ w_C \\ \Omega_x \\ \Omega_y \\ \Omega_z \end{bmatrix} \quad (6)$$

where  $x$ ,  $y$  and  $z$  are coordinates in the 3D space,  $u_X$ ,  $v_X$  and  $w_X$  are the displacements of a point X following axes  $\vec{x}$ ,  $\vec{y}$  and  $\vec{z}$ , and  $\Omega_x$ ,  $\Omega_y$  and  $\Omega_z$  are the interface rotation around the same axes. Following this approach, all interfaces dofs are eliminated from the global finite element model dofs list, thus reducing the computational cost of the structure model. In place of those eliminated dofs, each damper face is now represented by 6 dofs: 3 translational dofs and 3 rotational dofs (see Fig. 2).

### Model reduction of the core of the dampers

The method used here to reduce the damper finite element model combine the Craig-Bampton method (Craig and Bampton, 1983) and a multi-model approach (Rouleau *et al.*, 1994). In the case of a structure made of elastic and viscoelastic materials, the dynamic equation is given by equation (3). Following the Craig-Bampton method, boundary and internal dofs are separated. Here, the boundary dofs are the 12 dofs of the rigid interfaces noted  $\mathbf{u}_B$  and the internal dofs are the remaining dofs of the dampers noted  $\mathbf{u}_I$ . This leads to write equation (3) as:

$$\left( \begin{bmatrix} \mathbf{K}_{BB}^0 & \mathbf{K}_{BI}^0 \\ \mathbf{K}_{IB}^0 & \mathbf{K}_{II}^0 \end{bmatrix} + i\omega h^*(\omega) \begin{bmatrix} \mathbf{K}_{BB}^\infty & \mathbf{K}_{BI}^\infty \\ \mathbf{K}_{IB}^\infty & \mathbf{K}_{II}^\infty \end{bmatrix} - \omega^2 \begin{bmatrix} \mathbf{M}_{BB} & \mathbf{M}_{BI} \\ \mathbf{M}_{IB} & \mathbf{M}_{II} \end{bmatrix} \right) \begin{bmatrix} \mathbf{u}_B \\ \mathbf{u}_I \end{bmatrix} = \begin{bmatrix} \mathbf{f}_B \\ \mathbf{0} \end{bmatrix} \quad (7)$$

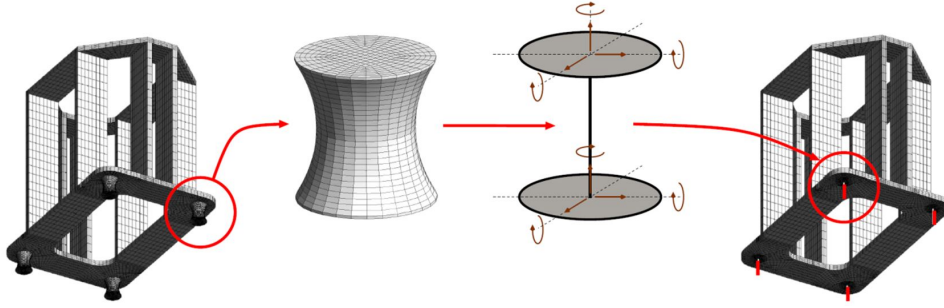


Figure 2 – Model reduction strategy considering elastomer damping devices

where the right-hand side is only composed of reaction forces  $\mathbf{f}_B$  at the interfaces. The first part of the reduced basis is composed of the static modes  $\Psi_{IB}$  which are defined by:

$$\Psi_{IB} = -(\mathbf{K}_{II}^0)^{-1} \mathbf{K}_{IB}^0 \quad (8)$$

The number of static modes is equal to the number of interfaces dofs, 12 in the present case. The second part of the reduced basis is composed of the eigenmodes of the fixed interface problem solutions of the following generalised :

$$(\mathbf{K}_{II}^0 + i\omega h^*(\omega) \mathbf{K}_{II}^\infty - \omega^2 \mathbf{M}_{II}) \mathbf{u}_I = \mathbf{0} \quad (9)$$

Solving equation (9) would lead to the vibration modes of the structure but due to the frequency dependence of the term  $i\omega h^*(\omega)$ , this eigenproblem is non-linear in frequency and can not be solved directly. The proposed solution is to use a multi-model approach. It has been often used to represent non-linear dynamic systems by interpolating locally linear models obtained from the sampling of the non-linear system. It has been applied by Rouleau *et al.* (1994) to build a projection basis representative of the complex non-linear eigenvalue of equation (9). The multi-model basis is here built by the combination of many smaller basis  $\Phi(\omega_d)$  and each of these basis is computed by solving the pseudo-eigenvalue problem (10) where only the real part of the equation is kept:

$$(\mathbf{K}_{II}^0 + \Re(i\omega_d h^*(\omega_d)) \mathbf{K}_{II}^\infty - \omega_d^2 \mathbf{M}_{II}) \Phi_k(\omega_d) = \mathbf{0} \quad (10)$$

where  $\omega_d$  values are chosen to sample the whole frequency range of interest. In any basis  $\Phi(\omega_d)$  the modes are independent but the modes from two different basis may be co-linear so a Gramm-Schmidt orthonormalisation algorithm is necessary. In the literature, two modal basis evaluated at the minimum and the maximum frequency of the range of interest combined with a static correction lead to a good approximation of the dynamic response of highly damped structures. This choice of  $\omega_{min}$  and  $\omega_{max}$  (i.e. lower and upper limits of the frequency band of interest) can be not optimal in specific problems but represents a pragmatic solution and will be validated in the numerical example. In this study, the static correction is already taken into account by the attachment modes of the static response, so only the modal basis at the minimum and maximum frequency need to be computed. Solving equation (10) for  $\omega_d = \omega_{min}$  and  $\omega_d = \omega_{max}$  lead to the two basis  $\Phi_{min}$  and  $\Phi_{max}$  which both respect the orthogonality conditions:

$$\Phi(\omega_d)^T \Re(\mathbf{K}_{II}(\omega_d)) \Phi(\omega_d) = \text{diag}(\omega_1^2, \dots, \omega_I^2) \quad \text{and} \quad (\omega_d)^T \mathbf{M}_{II} \Phi(\omega_d) = \mathbf{1}_I \quad (11)$$

where  $\omega_d$  stands for  $\omega_{min}$  or  $\omega_{max}$  and where:

$$\mathbf{K}_{II}(\omega_d) = \mathbf{K}_{II}^0 + i\omega_d h^*(\omega_d) \mathbf{K}_{II}^\infty \quad (12)$$

Both  $\Phi_{min}$  and  $\Phi_{max}$  diagonalize the  $\Re(\mathbf{K}_{II}(\omega_d))$  matrix but they don't diagonalize  $\mathbf{K}^0$  or  $\mathbf{K}^\infty$  and this will have an impact on the further condensation step. The dynamic of the system is then reduced by truncating the basis  $\Phi_{min}$  into  $\Phi_{Ip}$  and the basis  $\Phi_{max}$  into  $\Phi_{Iq}$  with  $p < I$  and  $q < I$ . The complete dynamic response is then obtained by combining the two truncated modal basis  $\Phi_{Ip}$  and  $\Phi_{Iq}$  into matrix  $\Phi_{Im}$ , with  $m = p + q < I$ .

By combining the static response coming from the behavior of structures connected to the damper's interfaces, and the dynamic response from the core of the damper, a complete reduced basis can be assembled in the form:

$$\begin{bmatrix} \mathbf{u}_B \\ \mathbf{u}_I \end{bmatrix} = \begin{bmatrix} \mathbf{I}_{BB} & \mathbf{0}_{Bm} \\ \Psi_{IB} & \Phi_{Im} \end{bmatrix} \begin{bmatrix} \mathbf{u}_B \\ \mathbf{q}_m \end{bmatrix} \quad (13)$$

The projection of equation (7) onto this reduced basis gives the following reduced system:

$$\left( \begin{bmatrix} \bar{\mathbf{K}}_{BB}^0 & \bar{\mathbf{K}}_{Bm}^0 \\ \bar{\mathbf{K}}_{mB}^0 & \bar{\mathbf{K}}_{mm}^0 \end{bmatrix} + i\omega h^*(\omega) \begin{bmatrix} \bar{\mathbf{K}}_{BB}^\infty & \bar{\mathbf{K}}_{Bm}^\infty \\ \bar{\mathbf{K}}_{mB}^\infty & \bar{\mathbf{K}}_{mm}^\infty \end{bmatrix} - \omega^2 \begin{bmatrix} \bar{\mathbf{M}}_{BB} & \bar{\mathbf{M}}_{Bm} \\ \bar{\mathbf{M}}_{mB} & \bar{\mathbf{M}}_{mm} \end{bmatrix} \right) \begin{bmatrix} \mathbf{u}_B \\ \mathbf{q}_m \end{bmatrix} = \begin{bmatrix} \mathbf{f}_B \\ \mathbf{0} \end{bmatrix} \quad (14)$$

where  $\bar{\mathbf{K}}_{mB}^\infty = (\bar{\mathbf{K}}_{Bm}^\infty)^T$  and  $\bar{\mathbf{M}}_{mB} = (\bar{\mathbf{M}}_{Bm})^T$ .

The details of the different terms of these reduced matrices are given by:

$$\bar{\mathbf{K}}_{BB}^0 = \mathbf{K}_{BB}^0 + \mathbf{K}_{BI}^0 \Psi_{IB} \quad (15)$$

$$\bar{\mathbf{K}}_{mB}^0 = \Phi_{Im}^T (\mathbf{K}_{IB}^0 + \mathbf{K}_{II}^0 \Psi_{IB}) \quad (16)$$

$$\bar{\mathbf{K}}_{mm}^0 = \Phi_{Im}^T \mathbf{K}_{II}^0 \Phi_{Im} \quad (17)$$

$$\bar{\mathbf{K}}_{BB}^\infty = \mathbf{K}_{BB}^\infty + \mathbf{K}_{BI}^\infty \Psi_{IB} + \Psi_{IB}^T \mathbf{K}_{IB}^\infty + \Psi_{IB}^T \mathbf{K}_{II}^\infty \Psi_{IB} \quad (18)$$

$$\bar{\mathbf{K}}_{mB}^\infty = \Phi_{Im}^T (\mathbf{K}_{IB}^\infty + \mathbf{K}_{II}^\infty \Psi_{IB}) \quad (19)$$

$$\bar{\mathbf{K}}_{mm}^\infty = \Phi_{Im}^T \mathbf{K}_{II}^\infty \Phi_{Im} \quad (20)$$

$$\bar{\mathbf{M}}_{BB} = \mathbf{M}_{BB} + \mathbf{M}_{BI} \Psi_{IB} + \Psi_{IB}^T \mathbf{M}_{IB} + \Psi_{IB}^T \mathbf{M}_{II} \Psi_{IB} \quad (21)$$

$$\bar{\mathbf{M}}_{mB} = \Phi_{Im}^T (\mathbf{M}_{IB} + \mathbf{M}_{II} \Psi_{IB}) \quad (22)$$

$$\bar{\mathbf{M}}_{mm} = \Phi_{Im}^T \mathbf{M}_{II} \Phi_{Im} \quad (23)$$

It is also important to note that due to the multi-model approach used in the computation of the dynamic response, a major difference arises between the method presented here and the usual Craig-Bampton: the classic method would results in null matrix in place of  $\bar{\mathbf{K}}_{mB}^\infty$  and the blocks  $\bar{\mathbf{K}}_{mm}$  and  $\bar{\mathbf{M}}_{mm}$  would be diagonals which is not the case here.

### Condensing the system on interfaces dofs

In order to further reduce the size of the system, it is proposed to condense the generalized unknowns  $\mathbf{q}_m$  on the boundary dofs. The second line of system (14) gives the following relation between the generalized coordinates  $\mathbf{q}_m$  and the interfaces displacements  $\mathbf{u}_B$ :

$$\mathbf{q}_m = -\mathbf{C}_{mB} \mathbf{u}_B \quad \text{with} \quad \mathbf{C}_{mB} = \left( \bar{\mathbf{K}}_{mm}^0 + i\omega h^*(\omega) \bar{\mathbf{K}}_{mm}^\infty - \omega^2 \bar{\mathbf{M}}_{mm} \right)^{-1} \left( \bar{\mathbf{K}}_{mB}^0 + i\omega h^*(\omega) \bar{\mathbf{K}}_{mB}^\infty - \omega^2 \bar{\mathbf{M}}_{mB} \right) \quad (24)$$

For the undamped case, the terms in the first parentheses are diagonal so the inversion is instantaneous, but in the damped case these terms are non-diagonal and the inversion adds some computation time. In order to limit this cost, it is possible to exploit the fact that the non-diagonal matrices are sparse. Replacing equation (24) into equation (14) leads to a condensed system on the interfaces which is equivalent to a super-element where its dimension is equal to the number of interface dofs (12 here):

$$\left( \mathbf{K}_{\text{super}}(\omega) - \omega^2 \mathbf{M}_{\text{super}}(\omega) \right) \mathbf{u}_B = \mathbf{f}_B \quad (25)$$

where the super-element mass and stiffness matrices are given by:

$$\mathbf{K}_{\text{super}}(\omega) = \bar{\mathbf{K}}_{BB}^0 + i\omega h^*(\omega) \bar{\mathbf{K}}_{BB}^\infty - \left( \bar{\mathbf{K}}_{Bm}^0 + i\omega h^*(\omega) \bar{\mathbf{K}}_{Bm}^\infty \right) \mathbf{C}_{mB} \quad (26)$$

$$\mathbf{M}_{\text{super}}(\omega) = \bar{\mathbf{M}}_{BB} - \bar{\mathbf{M}}_{Bm} \mathbf{C}_{mB} \quad (27)$$

### APPLICATION TO THE SUPPORT STRUCTURE MOUNTED ON 4 DAMPERS

A comparison between the reference full finite element model and the proposed super-element is made. An harmonic displacement is imposed on the structure lower interfaces, in a direction that is parallel to these interfaces: the dampers are not moving up and down but rather in a left-forward/right-backward kind of motion. The frequency range is chosen from 0 Hz to 500 Hz and the resulting displacements at observation point P (see Fig. (1)), for both the full reference model and the super-element, are plotted on Fig. (3). The displacement of point P for the full model without damping is also plotted to show that the chosen viscoelastic parameters lead to a well damped structure. Two types of modes (damper only or full structure) are shown in Fig. (4) and their frequencies are plotted in vertical line on Fig. (3).

One hundred modes are taken in the dynamic modal basis at null frequency in the multi-model approach. The high number of modes needed here is due to the same stiffness difference that is exploited for the kinematical constraint of the dampers interfaces: the stiffness of the elastomer core is so low that around a hundred modes are found in the frequency range 0-500 Hz. The frequency limit chosen for the calculation of this modal basis is 512 Hz, which is roughly equal to the max frequency of the frequency range, so the method is accurate.

For illustration purpose, mode shapes of the six attachment modes associated to the the lower interface of the elastomer devices are plotted on Fig. (5). Moreover, the shapes of the first four fixed-interface normal modes of the elastomer damping devices are plotted on Fig. (6).

For the second basis of the multi-model, the one that contains the pseudo-normal modes at the max frequency, only ten modes are needed to give a good approximation. This is due to the fact that pseudo-normal modes are computed from

Dynamic analysis of elastomer damping devices

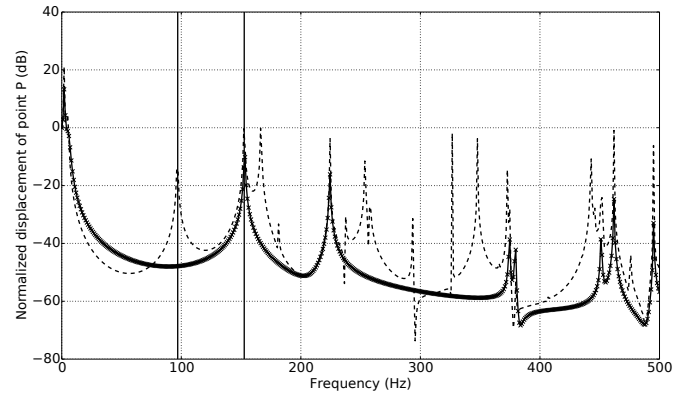


Figure 3 – Normalized displacement of point P (see Fig. 1) for the reference undamped model (dotted line), the reference damped (full line) and for the reduced model (cross-dotted line)

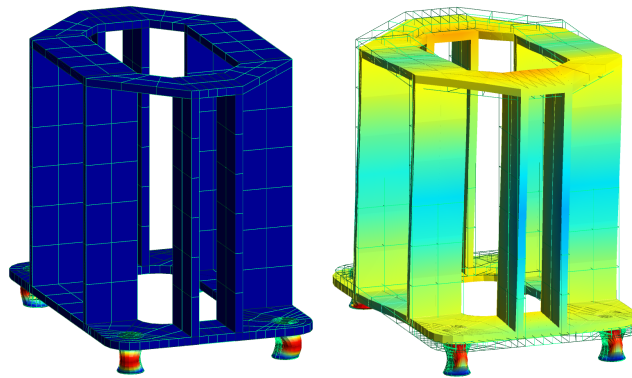


Figure 4 – Modes of the undamped full structure at 94 Hz and 151 Hz (see the vertical lines on figure 3)

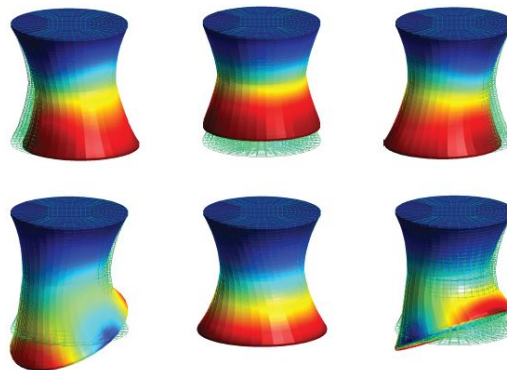


Figure 5 – Mode shapes of the attachment modes associated to the the lower interface of the elastomer devices

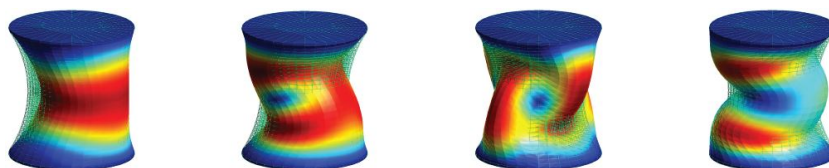


Figure 6 – Mode shapes of the first four fixed-interface normal modes of the elastomer damping devices (respectively at 96 Hz, 165 Hz, 231 Hz and 252 Hz)

the real part of the complex stiffness matrix at a given frequency. The real part of the complex modulus is greater than one thus adding stiffness to the system so a lower number of modes is present in the frequency range of interest. The frequency limit chosen for the calculation of this second modal basis is 580 Hz, which again is roughly equal to the max frequency of the frequency range.

As it can be seen on figure (3), the super-element matches the results of the reference model with a small error in displacement, thus validating the modified Craig-Bampton proposed in this work. The different computational times from both the FRF calculation of the reference model and the super-element are given in Table 3. The assembly of the super-element is done once for all, before the FRF calculation, and the corresponding computational times is given under the name of Pre CPU time in table 3. The sum of both the super-element assembly time and the FRF computational time of the modified Craig-Bampton is more than 10 times lower than the computational time of the reference model, thus validating the present super-element approach.

**Table 3 – Computational time of both the reference and super-element models.**

	Reference model	Super-element
Pre CPU time	-	23 min
FRF CPU time	14 h 40 min	51 min
total CPU time	14 h 40 min	1 h 14 min

## CONCLUSION

The aim of the presented method is to reduce the finite element model of a damper made of an elastomer core and aluminium faces to a 12 dofs super-element. This super-element is built through the combination of a kinematical constraint to enforce rigid body motion at the damper interfaces and a Craig-Bampton approach to reduce and condense the finite element dofs on the interfaces. A multi-model approach is used to keep the frequency dependence of the finite element model during the Craig-Bampton reduction process. The result is a 12 dofs super-element that replace the full finite element model. This super-element can be connected to any other finite element model through its interfaces nodes, each of them having three translational dofs and three rotational dofs.

To test this method, the case of an aluminum structure supported on four dampers is studied. A reference model, consisting in the structure and 4 non-reduced dampers, and a reduced model, made of the same structure with four super-elements, are compared. Displacements of one structural point are computed for both the reference and reduced models. The displacement responses are closed on the whole frequency range thus validating the proposed methodology. The computational times of both models are also investigated and show that the reduced model is more than 10 times faster to compute than the reference model. A library of super-elements corresponding to various damper geometries and materials can be built off-line through this approach and then be used for design and optimization purposes in a full model.

## REFERENCES

- Bagley, R.L. and Torvik. P.J., 1983, "A theoretical basis for the application of fractional calculus to viscoelasticity", *Journal of Rheology*, Vol. 27, No. 3, pp. 201-210.
- Craig, R.R., Bampton, M.C.C., 1968, "Coupling of substructures for dynamic analysis", *AIAA Journal*, Vol. 6, No. 7, pp. 1313-1319.
- Galucio, A.C., Deü, J.-F. and Ohayon, R., 2004, "Finite element formulation of viscoelastic sandwich beams using fractional derivative operators", *Computational Mechanics*, Vol. 33, No. 4, pp. 282-291.
- Hale, A.L., 1984, "Substructure synthesis and its iterative improvement for large nonconservative vibratory systems", *AIAA Journal*, Vol. 22, No. 2, pp. 265-272.
- Leung, A.Y.T., 1988, "Damped dynamic substructures", *International Journal for Numerical Methods in Engineering*, Vol. 26, No. 11, pp. 2355-2365.
- de Lima, A.M.G., da Silva, A.R., Rade, D.A. and Bouhaddi, N., 2010, "Component mode synthesis combining robust enriched Ritz approach for viscoelastically damped structures", *Eng. Struct.*, Vol. 32, No. 5, pp. 1479-1488.
- Morin, B., Legay, A. and Deü, J.-F., 2016, "Reduced Order Models for dynamic behavior of elastomer damping devices", *Proc. of the 12th Int. Conf. on Recent Advances in Structural Dynamics, RASD 2016*, Southampton, UK.
- Park, S.W., 2001, "Analytical modeling of viscoelastic dampers for structural and vibration control", *International Journal of Solids and Structures*, Vol. 38, No. 44-45, pp. 8065-8092.
- Rouleau, L., Deü, J.-F. and Legay, A., 2014, "Review of reduction methods based on modal projection for highly damped structures", *Proceedings of the 11th World Congress on Computational Mechanics, WCCM XI*, Barcelona, Spain.
- Rouleau, L., Deü, J.-F., Legay, A., Sigrist, J.-F. and Le Lay, F., 2012, "A component mode synthesis approach for dynamic analysis of viscoelastically damped structures", *Proceedings of the 10th World Congress on Computational Mechanics, WCCM 2012*, São Paulo, Brazil.

## RESPONSIBILITY NOTICE

The authors are the only responsible for the material included in this paper.